Research Paper

Genomic landscapes by multiregion sequencing combined with circulation tumor DNA detection contribute to molecular diagnosis in glioblastomas

Chao Yang[1,2], Yanli Tan[3,4], Shouwei Li[5], Junhu Zhou[1,2], Qixue Wang[1,2], Yunfei Wang[1,2], Yingbin Xie[8], Luyue Chen[6], Jie Li[7], Chuan Fang[8], Chunsheng Kang[1,2,9]

[1]Department of Neurosurgery, Tianjin Medical University General Hospital, Tianjin, China
[2]Laboratory of Neuro-Oncology, Tianjin Neurological Institute, Department of Neurosurgery, Tianjin Medical University General Hospital and Key Laboratory of Neurotrauma, Variation, and Regeneration, Ministry of Education and Tianjin Municipal Government, Tianjin, China
[3]Department of Pathology, Affiliated Hospital of Hebei University, Baoding, China
[4]Department of Pathology, Hebei University Medical College, Baoding, China
[5]Department of Neurosurgery, Beijing Sanbo Brain Hospital, Capital Medical University, Beijing, China
[6]Department of Neurosurgery, Zhongshan Hospital Xiamen University, Xiamen, Fujian, China
[7]ProteinT Biotechnologies, Co. Ltd., Tianjin, China
[8]Department of Neurosurgery, Affiliated Hospital of Hebei University, Baoding, China
[9]Affiliated Cancer Hospital and Institute of Guangzhou Medical University, Guangzhou, China

Correspondence to: Chuan Fang, Chunsheng Kang; **email:** fangchuan103@126.com, kang97061@tmu.edu.cn
Keywords: glioblastoma, intratumor heterogeneity, exon sequencing, ctDNA sequencing
Received: September 3, 2019 **Accepted:** November 18, 2019 **Published:** December 10, 2019

Copyright: Yang et al. This is an open-access article distributed under the terms of the Creative Commons Attribution License (CC BY 3.0), which permits unrestricted use, distribution, and reproduction in any medium, provided the original author and source are credited.

ABSTRACT

Glioblastoma is a highly aggressive brain malignancy with a poor prognosis. Its high intratumor heterogeneity contributes to therapeutic resistance, tumor progression and recurrence. We sequenced 31 loci in 11 patients with glioblastoma (including one patient with samples available from the primary and recurrent tumors) to determine the genetic basis and intratumor heterogeneity of glioblastoma. By analyzing the somatic mutations, known driver genes were identified, including EGFR, PTEN and TP53, and the MUC16 gene exhibited the highest mutation rate in the samples examined. Through an evolutionary analysis of the sequencing results, the EGFR p.L861Q mutation was determined to play a role in the progression from the primary tumor to a relapsing tumor in one patient. We analyzed 1403 genes in blood-derived ctDNA that were previously revealed to play a role in tumorigenesis and the progression of cancer. Somatic mutations identified through ctDNA sequencing that match the results of multipoint exon sequencing in tumor tissues were detected, such as EGFR p.L861Q. These findings provide new insights into the intratumor heterogeneity and evolution of glioblastoma. In addition, ctDNA detection in blood samples represents a convenient method to dynamically identify the genetic changes and new therapeutic targets during the treatment of glioblastoma.

INTRODUCTION

Glioma is the most common primary intracranial tumor in adults, among which glioblastoma multiforme (GBM) has the highest degree of malignancy and a poor prognosis, with average survival rate of less than 15 months and a 5-year survival rate of less than 10% [1]. Currently, glioma is primarily treated with surgical resection, radiation and chemotherapy. The concurrent addition of temozolomide (TMZ) to radiation as a chemotherapy adjuvant modestly improves survival among young patients with a good performance status

and has become the standard of care [2]. Despite the benefits of TMZ, tumors invariably recur, leading to a fatal outcome. Therefore, a more in-depth understanding of the occurrence and progression of glioma will be beneficial for the development of personalized treatment.

Extensive genetic diversity in GBM results in resistance to standardized treatment and a poor prognosis. Through a recent exploration at the genetic level, a new strategy for obtaining a better understanding of and improving GBM treatment was discovered and proposed [1]. In particular, individualized targeted therapy is selected for individual tumor mutations [3, 4]. Although this approach seeks to maximize the drug response and patient survival, the intratumor heterogeneity of GBM poses significant challenges [5–7]. Specifically, each tumor contains multiple clones with different genetic alterations, which will require strategies designed to therapeutically target multiple molecules [5, 8]. The detection of a single tumor locus may not accurately reflect the genetic characteristics of other tumor regions, rendering the traditional biopsy prone to errors and posing a significant challenge in cancer medicine [9].

Tumor heterogeneity has been used to describe various forms of tumor variability, including variations in the intertumoral mutation pattern, variations in intratumor histology and intratumor mutational polyclonality [10]. Spontaneous somatic cell mutations combined with the microenvironment for the evolutionary selection of tumor subclones will promote the growth of single cancer cells into complex and heterogeneous tumor masses [11]. During the evolution of clones, new mutations become more frequent as tumors progress, increasing the difficulty of treating these tumors. The poor prognosis of patients often indicates the progression of tumor heterogeneity [12–14].

Based on accumulating evidence, GBM can be further classified at the genomic level to reveal the evolution of tumors [5]. In addition, tumor fragments from the same patient can be divided into different GBM subtypes [6]. In the present study, subclones were detected in patients with GBM prior to treatment and new subclones appeared in the same patients after standardized treatment. We also describe a subset of tumor-associated genetic changes in blood-derived ctDNA.

RESULTS

Known driver gene mutations and significantly mutated genes (SMGs) in GBM samples

All point mutations were expressed in the following 6 forms: C>A(G>T), C>G(G>C), C>T(G>A), T>A(A>T), T>C(A>G), and T>G(A >C). Tumor samples and point mutation types were clustered according to the number of point mutations (Supplementary Figure 1A). As expected, we detected a point mutation variation in samples collected at different loci of the same original tumor, but in the patients with recurrent tumors (NO. 05-recurrent), the mutation variation was less than the original sample (NO. 05-primary) (Supplementary Figure 1A). The overall mutation pattern of GBM was dominated by C>T and G>A (Supplementary Figure 1A), particularly in recurrent samples (derived from NO. 05-recurrent).

We next identified the driver gene mutations in these GBM samples using the CGC513 (https://cancer.sanger.ac.uk/census), Bert Vogelstein125 [15] and SMG127 [16] driver mutation databases for comparison. We subsequently selected the top 50 driver gene mutations for mapping and observed higher mutation frequencies for MUC16 (a 19/31 ratio), EGFR (a 19/31 ratio) and PTEN (a 16/31 ratio) (Figure 1A). The IDH1 mutation was detected in two patients (NO. 03 and NO. 05-recurrent) at 18% (not shown in the figure). The MUC16 gene, also called CA125, was recently shown to play a pivotal role in promoting ovarian cancer growth and metastasis [17] and is associated with a higher tumor mutation load (TML), better survival outcomes and better immune response in patients with gastric cancer [18].

We also identified 55,992 SNVs from our exon sequencing of 31 GBM loci. High-frequency mutations in GBM were analyzed using MuSiC software [19] and the convolution test (CT), Fisher's test (Fisher's combined P-value test, FCPT), and the likelihood ratio test (LRT). If the false discovery rate (FDR) ≤ 0.2 in two of three tests, the gene was considered a high-frequency mutation. Sixty-seven SMGs, including EGFR, PTEN, VNN1, and ZSCAN23, were identified (the top 50 are shown in Figure 1B). We analyzed our SMG data with the PathScan module of MuSiC [19] software to perform a pathway enrichment analysis and obtain insights into the genetic alterations in canonical signaling pathways. The significantly enriched pathways of high-frequency mutated genes were revealed and included focal adhesion, axon guidance, NGF signaling and the cAMP signaling pathway, among others (Supplementary Figure 1B). In addition, heatmaps of SMGs in tumor-related pathways were used to observe the variations in the mutation frequencies (Supplementary Figure 2). Again, we observed intratumor heterogeneity in the mutations in genes involved in these pathways associated with tumor formation and progression.

MUC16, the gene with the highest mutation frequency, indicates a good prognosis

We counted the gene mutations obtained from multipoint sequencing in 11 patients, and the 10 genes

with the highest mutation frequencies were MUC16, FAT1, EGFR, PTEN, ZFHX3, FAT4, FAT3, TSC1, ARHGAP5 and ATRX (Figure 1C). FAT1, FAT3 and FAT4 are cadherin family members, and this family of molecules is likely to be important in mammalian developmental processes and cell communication [20]. The loss of FAT1 also contributes to the mechanism of resistance mediated by CDK4/6i in ER^+ breast cancer [21]. EGFR, PTEN and ATRX are commonly mutated genes in glioma [1]. Multipoint sequencing can identify new high-frequency mutated genes in GBM. By analyzing the GO biological processes of genes that were mutated in more than three patients, we mainly observed enrichment in double-strand break repair, histone modification and phosphatidylinositol-mediated signaling, among other processes (Figure 1D).

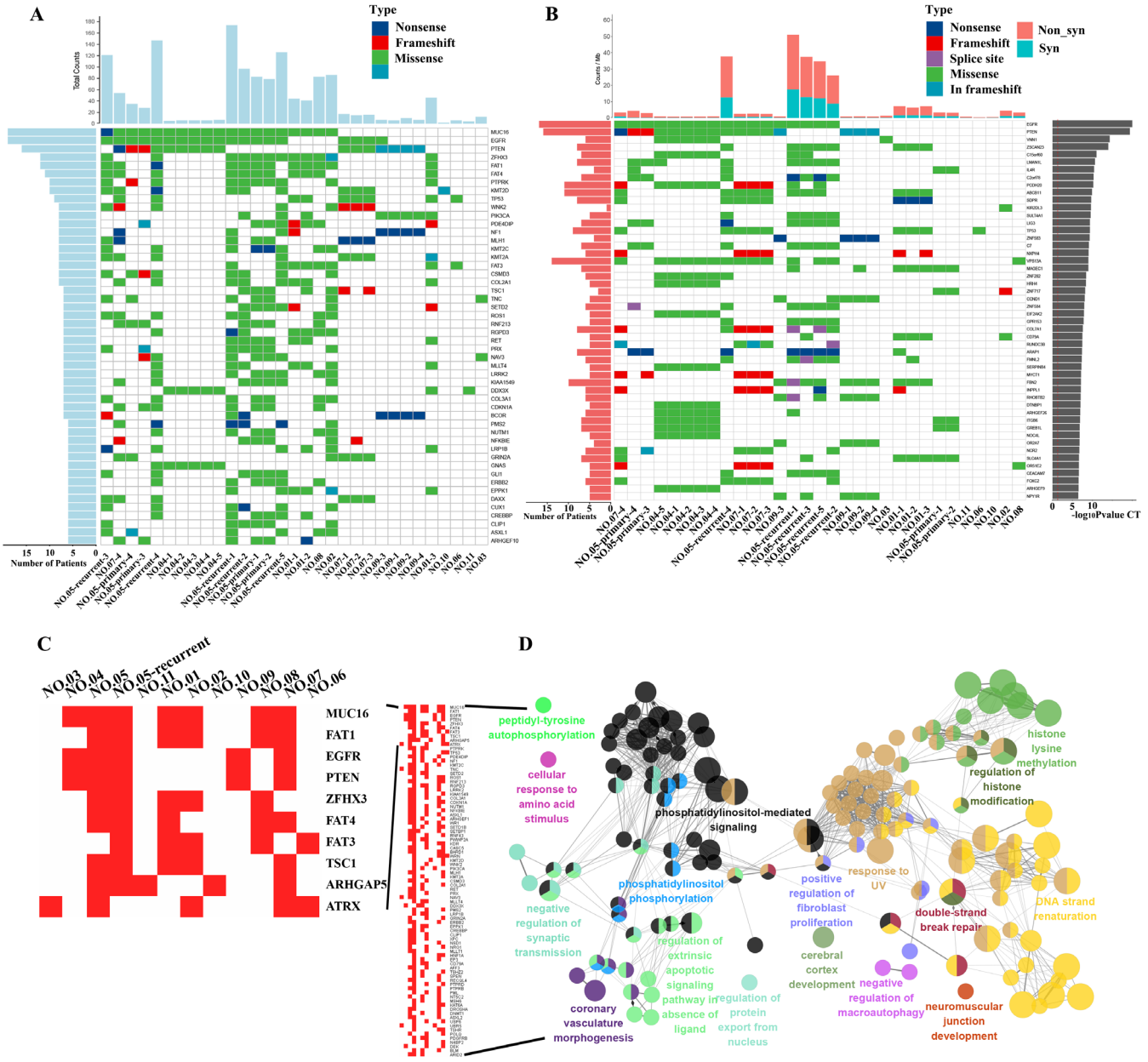

Figure 1. Driver gene mutation analysis and significantly mutated genes (SMGs) in GBM. (**A**) The top 50 driver genes with the highest mutation frequencies were selected for inclusion in the heat maps. The abscissa lists the sample names and the ordinate lists the gene names. The left graph shows the number of mutant samples and the top graph shows the number of mutated genes in each sample. (**B**) The graph on the right shows the log10 P-value of each gene mutation. The heat map (middle panel) presents gene mutations in GBM samples. The graph on the left shows the mutation frequency in the GBM samples examined. The mutant load is shown on the top of the heat map. (**C**) Mutation heatmap. (**D**) GO analysis.

Few mutations were identified in MUC16 in primary GBM samples, but a 15 percent mutation frequency was observed in recurrent GBM (Figure 2A–2B) in the CGGA (Chinese Glioma Genome Atlas) GBM database, validating our results. This finding indicates the importance of MUC16 in GBM recurrence. The most frequently mutated gene, MUC16, in our sequencing data also contains multiple mutation sites in the gene mutation data provided by TCGA (Figure 2C). By analyzing the TCGA clinical data, the overall survival curve showed that patients with GBM carrying a mutation in the MUC16 gene had a poor survival outcome (Figure 2D). Based on these results, multipoint sampling is a better indicator of underlying tumor progression.

Analysis of subclones and the evolution of primary and recurrent GBM samples from the same patient

We next outperformed a subclone analysis of primary and recurrent GBM samples from patient NO. 05 with the aim of exploring the genetic evolution of GBM.

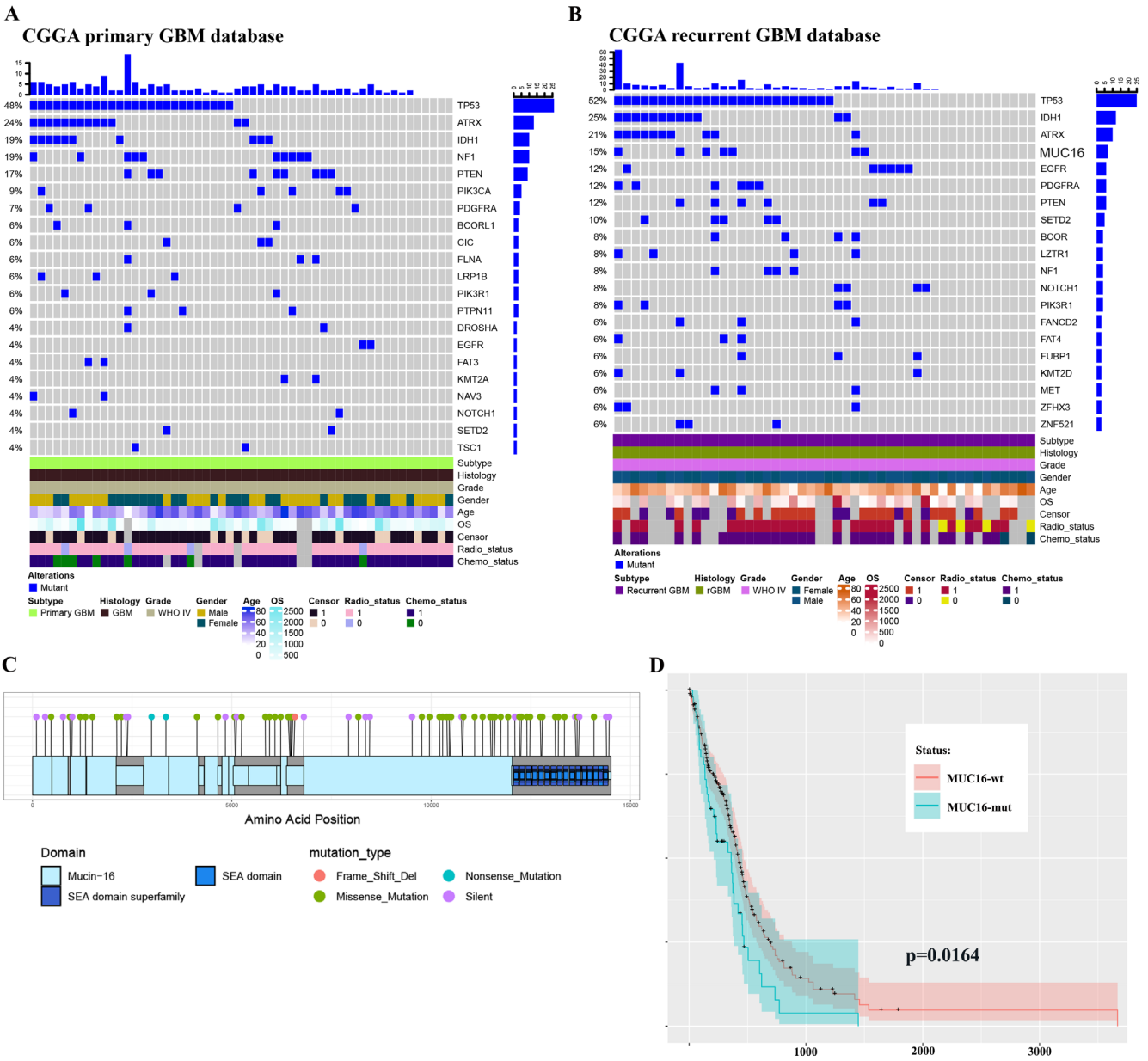

Figure 2. Multipoint sequencing provides a new map of mutations. (**A**–**B**) Genes that were mutated in the patient cohort were detected in CGGA primary and recurrent GBM WES databases. (**C**) MUC16 mutations in the TCGA database. (**D**) Survival curves of patients carrying wild type and mutant MUC16.

Multiple subclones were detected in each site of primary and recurrent tumor samples from patient NO. 05, but the mutated genes and frequency between tumor sites differed (Figure 3A and 3B). Clone 0 was present at a higher proportion in all sites, but clone 4 was present at a higher proportion in pri1 (NO. 05-primary 1) and pri2 (NO. 05-primary 2). Notably, clone 6 accounted for a higher VAF in all recurrent samples (Figure 3B–3D), suggesting that the gene mutations present in clone 6 play an important role in GBM recurrence. Further analysis using Pyclone CCF package ClonEvol [22] revealed the evolutionary relationship between the primary and recurrent GBM tumors in patient NO. 05 (Figure 3E). An analysis of the

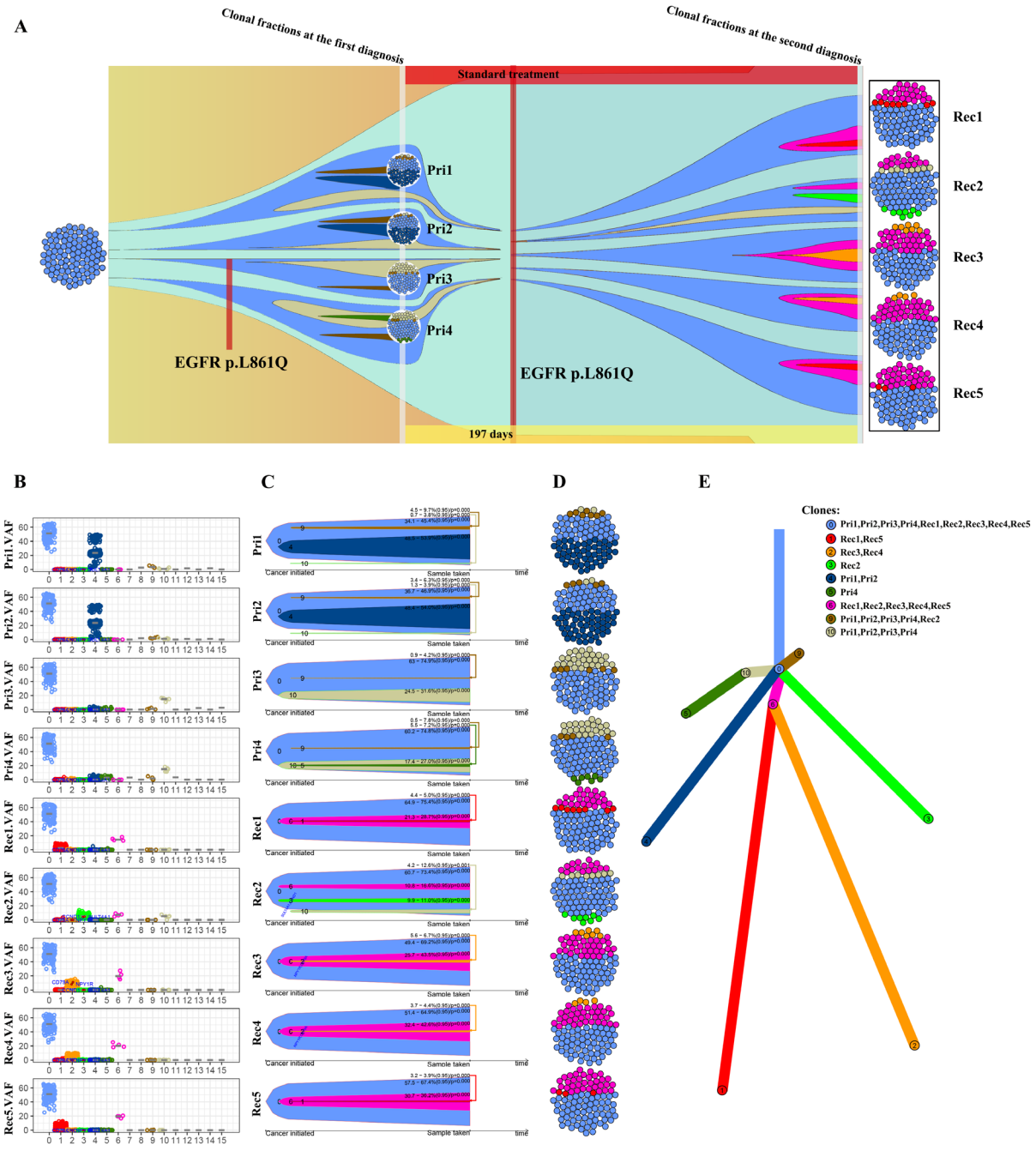

Figure 3. Analysis of the subclones and evolution of primary and recurrent GBM samples from patient NO. 05. (**A**) Four intra-tumor loci from the primary tumor and 5 intra-tumor loci from the recurrent tumor from the same patient were sequenced and analyzed. (**B**) VAF distribution of different subclone types at each intratumor locus. (**C**) A clonal evolution map of each intratumor locus. (**D**) Clonal structure distribution of each intratumor locus. (**E**) A tumorigenic chart of intratumor loci.

subclones and evolutionary relationship in patients NO. 05 and NO. 04 (Supplementary Figure 3) indicated that different branches appeared during GBM progression, and a complex pattern of intratumor heterogeneity gradually formed in these tumors. H&E (Supplementary Figure 4) and immunofluorescence staining (Supplementary Figure 5) of the tumors from patient NO. 05 also revealed significant intratumor differences.

The ctDNA in the blood predicts the overall genetic information of the GBM

The ctDNA in the blood carries the genetic information of the tumor and has become an indicator of the occurrence and progression of tumors following a liquid biopsy [23–25]. Because of the limited amount of ctDNA in the blood, we were unable to detect all genetic mutations identified in the tumors. In this study, we selected 1,403 common genes, which are known to be involved in tumor progression, and detected their common mutation sites for evaluation in ctDNA. Importantly, the EGFR p.L861Q mutation in the ctDNA of patient NO. 05 was detected in all recurrent samples but only in some of the original samples (Figure 4). By comparing the ctDNA sequencing data with tumor tissue exon sequencing results from all 11 patients with GBM and the TCGA gene mutation database, ctDNA sequencing detected common gene mutations in GBM

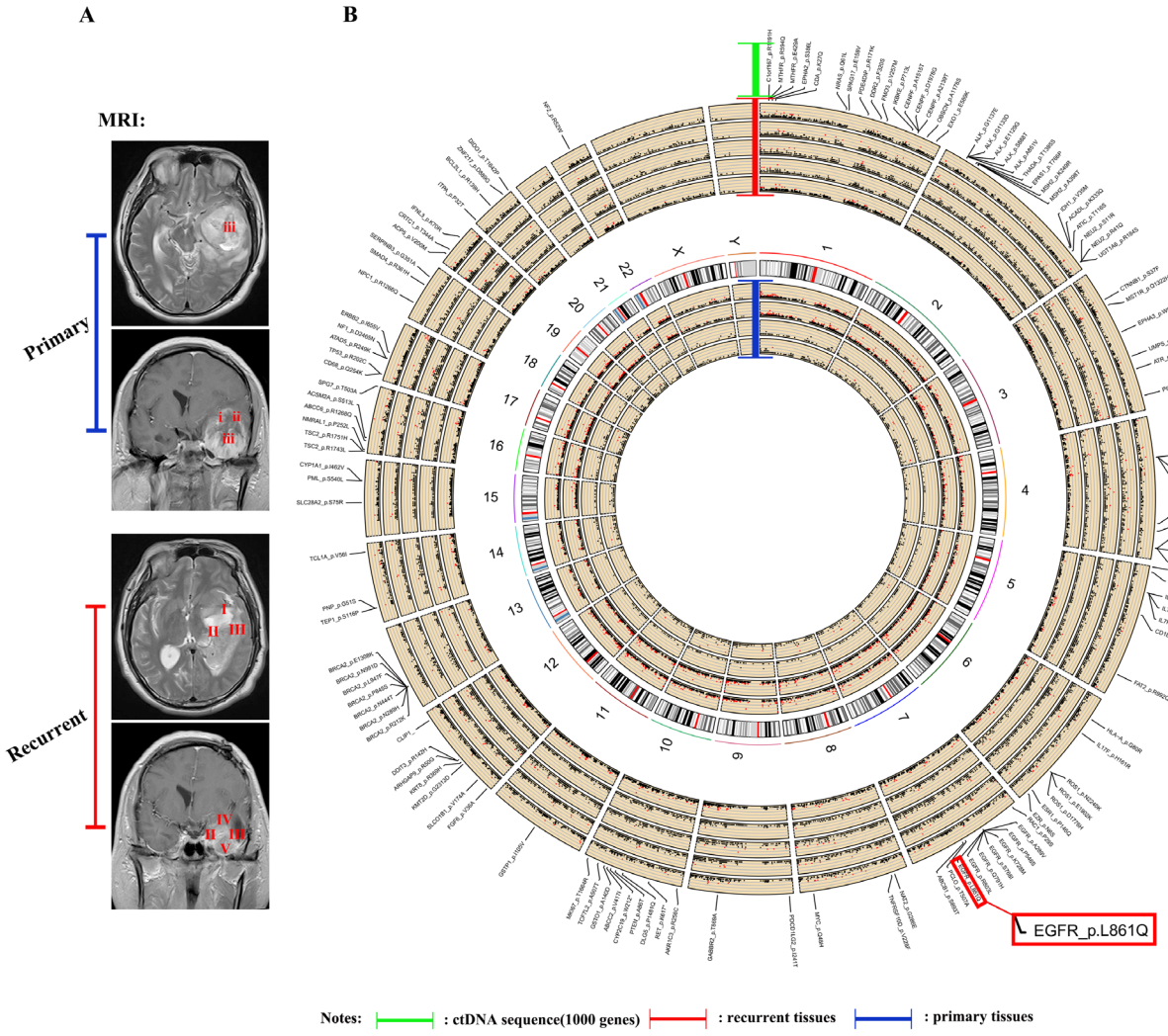

Figure 4. Sequencing and analysis of the ctDNA. (**A**) Magnetic resonance images show the different locations of tissue samples derived from patient NO. 05. (**B**) SNP density circos map of the primary and recurrent GBM samples from patient NO. 05. The first circle represents sample (**i**), the second circle represents sample (**ii**), the third circle represents sample (**iii**), the fourth circle represents the repeat of sample (**iii**), the fifth circle represents chromosomes, the sixth circle represents sample (**I**), the seventh circle represents sample (**II**), the eighth circle represents sample (**III**), the ninth circle represents sample (**IV**), the tenth circle represents sample (**V**), and the eleventh circle represents gene mutations detected using ctDNA testing.

tumors (Figures 5A–5C, Supplementary Figure 6 and Supplementary Figure 7) and obtained additional gene mutation information that failed to be detected in tumor tissue samples (Figure 5B and 5C).

DISCUSSION

GBM shows obvious molecular heterogeneity and invasive behavior [5, 7, 10, 26]. The heterogeneity of a tumor refers to the genetic changes in its subpopulations of cells after multiple division sand proliferation during tumor growth [5, 6, 11, 27–30]. Following the development of new detection technology, the most recent data, including next-generation sequencing data, support the clonal evolution model as the main theoretical basis of heterogeneity [30–32]. By sequencing 31 intratumor loci and ctDNAs from 11 patients with primary and recurrent GBM, we observed high intratumor heterogeneity at the levels of both somatic gene mutations and chromosomal copy numbers

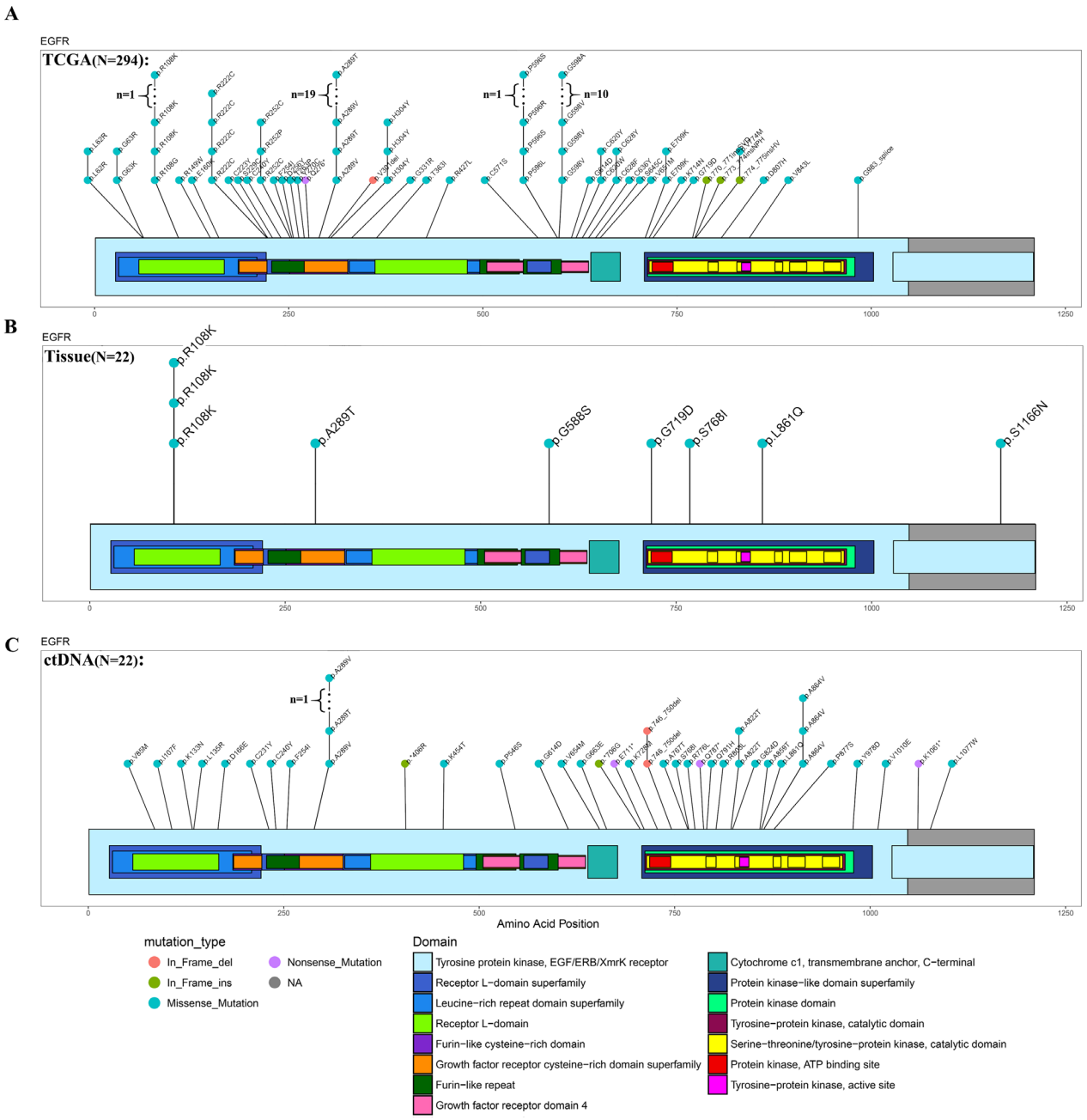

Figure 5. Comparison of EGFR mutations identified using ctDNA and tumor DNA sequencing. (**A**–**C**) Mutation hotspots of EGFR mutations present in the TCGA database, patient tissue WES data and ctDNA testing results.

in the present study. The intratumor heterogeneity of GBM has been suggested to contribute to therapeutic resistance [33], tumor progression and recurrence [34]. Interestingly, even recurrent GBM presented a high degree of genetic heterogeneity in the present study. Moreover, the subclone analysis revealed different signatures of intratumor heterogeneity between primary and recurrent GBM (Figure 3A–3C). For instance, clone 6 was only present in recurrent tumors (Figure 3B), suggesting that it may represent a causal factor of recurrent GBM that is more refractory to treatment than the primary tumor. These results suggest the selective evolution of the tumor subclone structure after treatment (Figure 3A). Further investigations of the underlying detailed molecular changes and driving force of the heterogeneity in recurrent GBM might substantially improve the therapeutic efficacy and prognosis of GBM.

Additional treatment strategies for GBM are urgently needed. Precision medicine has been a major focus in the field, with the goal of matching specific tumor mutations with potential therapeutic drugs to provide individualized treatment options [35, 36]. An increasing number of studies have identified a number of driver gene mutations, including TP53, PTEN, EGFR, PIK3CA, ATRX, IDH1, PIK3R1, and PDGFRA, MSH6 and PRDM2, in GBM [1, 37, 38]. Consistent with these findings, frequent mutations in these known driver genes were detected in our GBM samples (Figure 1A and 1C). In the present study, MUC16 was the most frequently mutated known driver gene in the GBM tissue samples sequenced (Figure 1A). Studies of MUC16 in other tumor types have indicated that MUC16 is a critical therapeutic target [17, 18]. For instance, an antibody (DUC5754A) against MUC16 has been advanced to a phase 1 clinical trial for ovarian cancer [39]. In addition, we detected the EGFR p.L861Q mutation in all intratumor loci in recurrent tumors but in a few loci in primary GBM tumors from patient NO. 05, suggesting that the EGFR p.L861Q mutation potentially represents a marker for predicting recurrence.

Based on accumulating evidence, ctDNA, which is released into the blood after the apoptosis of tumor cells, has potential as a tumor biomarker [40–43]. Moreover, ctDNA provides a comprehensive picture of the tumor genome, as it reflects the DNA released from multiple tumor regions [44–47]. Recently, ctDNA has been detected in the cerebrospinal fluid (CSF) from patients with brain malignancies [44]. Compared to ctDNA testing, single-site biopsy or several reliable biopsies are needed to obtain the same amount of genetic information [44–47]. However, ctDNA also has some substantial limitations, such as the generally very low level of ctDNA in plasma, resulting in a small range of genes that are able to be detected using sequencing [48]. In the present study, we selected 1,403 genes involved in tumorigenesis and progression for detection and compared them with the sequencing results obtained from intratumor loci. Importantly, the information obtained from the analysis was highly consistent with the findings from the sequencing of intratumor loci (Figures 4 and 5). Thus, blood-derived ctDNA can be used as a liquid biopsy to help diagnose and monitor GBM.

Our study has provided a better understanding of intratumor heterogeneity, disease progression and recurrence in patients with GBM. Our analysis of the temporal sequence of mutations and chromosomal copy number revealed genetic forces acting on the cancer genome and provided new insights into the patterns and dynamics of tumor evolution. Further investigations will provide more detailed descriptions of the mechanisms of disease relapse and new therapeutic strategies for this disease.

MATERIALS AND METHODS

Blood specimen collection and preservation

Streck noninvasive blood vessel collection tubes (218962, 10 mL, cell-free DNA BCT) were used to collect venous blood prior to surgery. The supernatant and cell pellet were separately preserved after centrifugation. The first centrifugation was conducted at 1600 × g for 10 minutes at 4°C. The blood cell pellet was collected after centrifugation and stored at -80°C. The upper plasma fraction was subjected to a second centrifugation step (4°C, 16000 × g, 10 minutes). The upper plasma fraction produced after second centrifugation step was collected and stored at -80°C.

Clinical samples

Our study was approved by the Ethics Committee of the Affiliated Hospital of Hebei University (HDFY-KL-LL-2018-17). All tissues were stored in liquid nitrogen for whole exome sequencing (WES). Clinical data for the tumor samples used in this study are listed in the supplementary table (Supplementary Table 1).

DNA sequencing

Qualified tissue and blood cell DNA samples were randomly disrupted into 150- to 220-bp fragments by Covaris, and then the Agilent SureSelect Human All Exon V6/V7 kit was used for library construction and capture. The captured library was subjected to whole-exome sequencing to identify somatic mutations, including single nucleotide variants (SNVs), insertions or deletions (INDELs), and copy number alterations

(CNAs). A 100X target coverage of coding bases in the exome was achieved for all samples.

The ctDNA was extracted from the upper centrifugal plasma of patients. A captured ctDNA library was then constructed. The purified library was sequenced using a NovaSeq 6000 sequencer. The ctDNA sequencing method was based on next-generation high-throughput sequencing (NGS) and designed to detect a variety of solid tumor- and drug-related gene mutations. The panel design adopted Roche NimbleGen SeqCap probe design technology and covered hot spots, drug-related mutations and key areas of 1403 genes to ensure the comprehensive detection of hot spots and rare and unknown mutation sites to the maximum extent and to ensure that valuable mutation information for patients was not ignored.

Bioinformatics analyses and statistical analyses

The caner genome atlas (TCGA) somatic mutation (SNPs and small INDELs) data used in this study were retrieved from the following website: https://xena.ucsc.edu/welcome-to-ucsc-xena/. CGGA [49] WES sequencing results were analyzed using the website: http://cgga.org.cn/index.jsp. GO and survival analyses were performed using the R package Clusterprofiler [12] and survminer v0.2.1 (https://www.rdocumentation.org/packages/survminer). The mutation hotspot graphic was generated using the R package GenVisR [13]. The genome circos map was produced using the R package Rcircos [14] (https://www.rdocumentation.org/packages/RCircos). The nonredundant biological terms for large clusters of genes in a functionally grouped network were visualized using the Cytoscape plug-in clueGO [50].

Somatic SNV test

SNV is defined as a single nucleotide variant, which refers to the variation caused by the replacement of a single nucleotide in the genome. We used MuTect [51] software to search for somatic SNVs and annotated the results with Annovar software.

Somatic INDELs/SNVs/SVs

The Somatic INDEL sites were detected using Strelka [52] and annotated using Annovar software. We used Control-FREEC [53] and lumpy [54] to detect somatic CNVs and SVs in paired samples of tumor and normal tissues.

Somatic mutations

The mutation spectrum and mutation signature were analyzed. All point mutations were reported in the following 6 forms: C>A(G>T), C>G(G>C), C>T(G>A), T>A(A>T), T>C(A>G), and T>G(A>C). Tumor samples and point mutation types were clustered according to the number of point mutations. The preference of point mutation types and the degree of similarity of each tumor sample were studied. Mutation characteristics were analyzed to extract the mutation features of somatic point mutations based on the number of 96 point mutations in various tumor samples and using non-negative Matrix Factorization (NMF) [55]. Each mutation feature reflects the physical, chemical or biological process of a cancer somatic mutation. The COSMIC web site lists more than 30 known mutations.

Driver mutations

We compared somatic cell variations with known driver genes and screened known driver genes in these tumor samples. The driver genes used for comparison were derived from the following sites:

(1) CGC513: the driver genes listed in the Cancer Gene Census (https://cancer.sanger.ac.uk/census);

(2) Bert Vogelstein125: 125 mut-driver genes in the paper by Bert Vogelstein and colleagues [15];

(3) SMG127: significant mutated genes identified in pan-cancer data [16].

Significantly mutated genes (SMGs)

High frequency mutations in tumors were analyzed using MuSiC [19] software. MuSiC sets somatic cell mutations in all tumor samples as the background, performs statistical tests on various mutation types in genes, and detects genes with a significantly higher mutation frequency than the background mutation rate. MuSiC software performs the SMG test using three methods, including a convolution test (CT), Fisher's test (Fisher's combined P-value test, FCPT), and likelihood ratio test (LRT). If FDR $\leq$ 0.2 in two inspections, the gene will be categorized as a high-frequency mutation. PathScan [56] (a module of MuSic) was used to analyze high-frequency mutated genes. The metabolic pathway databases used for enrichment were KEGG, PID and Reactome.

Evolutionary tree analysis

According to the mutation frequency identified in somatic sites as the Vaf (variant allele frequency) combined with copy number variations, Pyclone software was used to calculate the proportion of mutant cells in the CCF (cancer cell fraction) of tumor and

studied the clone structures. ClonEvol [22] software was employed to analyze the evolutionary relationship between tumor samples.

H&E staining, immunofluorescence staining, and confocal imaging

Paraffin-embedded tissue sections were used for H&E staining. For immunofluorescence staining, the sections were incubated with primary antibodies (1:100 dilution) (p-EGFR and POLK, from CST Cell Signaling Technology) overnight at 4°C, followed by a 1-h incubation with a fluorescently labeled secondary antibody (1:100 dilution) at 37°C. Images were obtained with a confocal microscope (Olympus FluoView 1200 system). All confocal scanning parameters were maintained at constant values between samples, and the images were minimally processed to maintain the integrity of the data.

Abbreviations

SMGs: significantly mutated genes; ctDNA: circulating tumor DNA; SNV: single-nucleotide variant; CTX: interchromosomal translocation; ITX: intrachromosomal translocation; INS: inversion; DEL: deletion; DUP: tandem duplication and INV: inversion.

CONFLICTS OF INTEREST

The authors declare no competing financial interests.

FUNDING

This study was supported by the National Natural Science Foundation of China (81772667), Beijing Tianjin Hebei Basic Research Cooperation Project (18JCZDJC45500, H2018201306), Training Program for Young Talents of Fujian Health System (2017-ZQN-90), Natural Science Foundation of Fujian Province (2018J01399), and the Tianjin Municipal Science and Technology Commission Project (15ZXLCSY00060, 15ZXJZSY00040). Validation of the WES sequencing was performed using a cohort retrieved from the CGGA database (http://cgga.org.cn/index.jsp).

REFERENCES

1. Brennan CW, Verhaak RG, McKenna A, Campos B, Noushmehr H, Salama SR, Zheng S, Chakravarty D, Sanborn JZ, Berman SH, Beroukhim R, Bernard B, Wu CJ, et al, and TCGA Research Network. The somatic genomic landscape of glioblastoma. Cell. 2013; 155:462–77. https://doi.org/10.1016/j.cell.2013.09.034 PMID:24120142

2. Stupp R, Mason WP, van den Bent MJ, Weller M, Fisher B, Taphoorn MJ, Belanger K, Brandes AA, Marosi C, Bogdahn U, Curschmann J, Janzer RC, Ludwin SK, et al, and European Organisation for Research and Treatment of Cancer Brain Tumor and Radiotherapy Groups, and National Cancer Institute of Canada Clinical Trials Group. Radiotherapy plus concomitant and adjuvant temozolomide for glioblastoma. N Engl J Med. 2005; 352:987–96. https://doi.org/10.1056/NEJMoa043330 PMID:15758009

3. I.H.P.r. April, Global Oncology Trends 2017, IMS Health website.

4. Stupp R, Hegi ME, Mason WP, van den Bent MJ, Taphoorn MJ, Janzer RC, Ludwin SK, Allgeier A, Fisher B, Belanger K, Hau P, Brandes AA, Gijtenbeek J, et al, and European Organisation for Research and Treatment of Cancer Brain Tumour and Radiation Oncology Groups, and National Cancer Institute of Canada Clinical Trials Group. Effects of radiotherapy with concomitant and adjuvant temozolomide versus radiotherapy alone on survival in glioblastoma in a randomised phase III study: 5-year analysis of the EORTC-NCIC trial. Lancet Oncol. 2009; 10:459–66. https://doi.org/10.1016/S1470-2045(09)70025-7 PMID:19269895

5. Vinci M, Burford A, Molinari V, Kessler K, Popov S, Clarke M, Taylor KR, Pemberton HN, Lord CJ, Gutteridge A, Forshew T, Carvalho D, Marshall LV, et al. Functional diversity and cooperativity between subclonal populations of pediatric glioblastoma and diffuse intrinsic pontine glioma cells. Nat Med. 2018; 24:1204–15. https://doi.org/10.1038/s41591-018-0086-7 PMID:29967352

6. Sottoriva A, Spiteri I, Piccirillo SG, Touloumis A, Collins VP, Marioni JC, Curtis C, Watts C, Tavaré S. Intratumor heterogeneity in human glioblastoma reflects cancer evolutionary dynamics. Proc Natl Acad Sci USA. 2013; 110:4009–14. https://doi.org/10.1073/pnas.1219747110 PMID:23412337

7. Bonavia R, Inda MM, Cavenee WK, Furnari FB. Heterogeneity maintenance in glioblastoma: a social network. Cancer Res. 2011; 71:4055–60. https://doi.org/10.1158/0008-5472.CAN-11-0153 PMID:21628493

8. Ene CI, Fine HA. Many tumors in one: a daunting therapeutic prospect. Cancer Cell. 2011; 20:695–97. https://doi.org/10.1016/j.ccr.2011.11.018 PMID:22172718

9. Marusyk A, Almendro V, Polyak K. Intra-tumour heterogeneity: a looking glass for cancer? Nat Rev

Cancer. 2012; 12:323–34.
https://doi.org/10.1038/nrc3261 PMID:22513401

10. Furnari FB, Cloughesy TF, Cavenee WK, Mischel PS. Heterogeneity of epidermal growth factor receptor signalling networks in glioblastoma. Nat Rev Cancer. 2015; 15:302–10.
https://doi.org/10.1038/nrc3918 PMID:25855404

11. Nowell PC. The clonal evolution of tumor cell populations. Science. 1976; 194:23–28.
https://doi.org/10.1126/science.959840 PMID:959840

12. Yu G, Wang LG, Han Y, He QY. clusterProfiler: an R package for comparing biological themes among gene clusters. OMICS. 2012; 16:284–87.
https://doi.org/10.1089/omi.2011.0118
PMID:22455463

13. Skidmore ZL, Wagner AH, Lesurf R, Campbell KM, Kunisaki J, Griffith OL, Griffith M. GenVisR: Genomic Visualizations in R. Bioinformatics. 2016; 32:3012–14.
https://doi.org/10.1093/bioinformatics/btw325
PMID:27288499

14. Zhang H, Meltzer P, Davis S. RCircos: an R package for Circos 2D track plots. BMC Bioinformatics. 2013; 14:244.
https://doi.org/10.1186/1471-2105-14-244
PMID:23937229

15. Kandoth C, McLellan MD, Vandin F, Ye K, Niu B, Lu C, Xie M, Zhang Q, McMichael JF, Wyczalkowski MA, Leiserson MD, Miller CA, Welch JS, et al. Mutational landscape and significance across 12 major cancer types. Nature. 2013; 502:333–39.
https://doi.org/10.1038/nature12634 PMID:24132290

16. Vogelstein B, Papadopoulos N, Velculescu VE, Zhou S, Diaz LA Jr, Kinzler KW. Cancer genome landscapes. Science. 2013; 339:1546–58.
https://doi.org/10.1126/science.1235122
PMID:23539594

17. Felder M, Kapur A, Gonzalez-Bosquet J, Horibata S, Heintz J, Albrecht R, Fass L, Kaur J, Hu K, Shojaei H, Whelan RJ, Patankar MS. MUC16 (CA125): tumor biomarker to cancer therapy, a work in progress. Mol Cancer. 2014; 13:129.
https://doi.org/10.1186/1476-4598-13-129
PMID:24886523

18. Li X, Pasche B, Zhang W, Chen K. Association of MUC16 Mutation With Tumor Mutation Load and Outcomes in Patients With Gastric Cancer. JAMA Oncol. 2018; 4:1691–98.
https://doi.org/10.1001/jamaoncol.2018.2805
PMID:30098163

19. Dees ND, Zhang Q, Kandoth C, Wendl MC, Schierding W, Koboldt DC, Mooney TB, Callaway MB, Dooling D, Mardis ER, Wilson RK, Ding L. MuSiC: identifying mutational significance in cancer genomes. Genome Res. 2012; 22:1589–98.
https://doi.org/10.1101/gr.134635.111
PMID:22759861

20. Dunne J, Hanby AM, Poulsom R, Jones TA, Sheer D, Chin WG, Da SM, Zhao Q, Beverley PC, Owen MJ. Molecular cloning and tissue expression of FAT, the human homologue of the Drosophila fat gene that is located on chromosome 4q34-q35 and encodes a putative adhesion molecule. Genomics. 1995; 30:207–23.
https://doi.org/10.1006/geno.1995.9884
PMID:8586420

21. Li Z, Razavi P, Li Q, Toy W, Liu B, Ping C, Hsieh W, Sanchez-Vega F, Brown DN, Da Cruz Paula AF, Morris L, Selenica P, Eichenberger E, et al. Loss of the FAT1 Tumor Suppressor Promotes Resistance to CDK4/6 Inhibitors via the Hippo Pathway. Cancer Cell. 2018; 34:893–905.e8.
https://doi.org/10.1016/j.ccell.2018.11.006
PMID:30537512

22. Dang HX, White BS, Foltz SM, Miller CA, Luo J, Fields RC, Maher CA. ClonEvol: clonal ordering and visualization in cancer sequencing. Ann Oncol. 2017; 28:3076–82.
https://doi.org/10.1093/annonc/mdx517
PMID:28950321

23. Beaver JA, Jelovac D, Balukrishna S, Cochran R, Croessmann S, Zabransky DJ, Wong HY, Toro PV, Cidado J, Blair BG, Chu D, Burns T, Higgins MJ, et al. Detection of cancer DNA in plasma of patients with early-stage breast cancer. Clin Cancer Res. 2014; 20:2643–50.
https://doi.org/10.1158/1078-0432.CCR-13-2933
PMID:24504125

24. Chabon JJ, Simmons AD, Lovejoy AF, Esfahani MS, Newman AM, Haringsma HJ, Kurtz DM, Stehr H, Scherer F, Karlovich CA, Harding TC, Durkin KA, Otterson GA, et al. Circulating tumour DNA profiling reveals heterogeneity of EGFR inhibitor resistance mechanisms in lung cancer patients. Nat Commun. 2016; 7:11815.
https://doi.org/10.1038/ncomms11815
PMID:27283993

25. Lavon I, Refael M, Zelikovitch B, Shalom E, Siegal T. Serum DNA can define tumor-specific genetic and epigenetic markers in gliomas of various grades. Neuro Oncol. 2010; 12:173–80.
https://doi.org/10.1093/neuonc/nop041
PMID:20150384

26. Gerlinger M, Rowan AJ, Horswell S, Math M, Larkin J, Endesfelder D, Gronroos E, Martinez P, Matthews N,

Stewart A, Tarpey P, Varela I, Phillimore B, et al. Intratumor heterogeneity and branched evolution revealed by multiregion sequencing. N Engl J Med. 2012; 366:883–92.
https://doi.org/10.1056/NEJMoa1113205
PMID:22397650

27. Yan HH, Siu HC, Law S, Ho SL, Yue SS, Tsui WY, Chan D, Chan AS, Ma S, Lam KO, Bartfeld S, Man AH, Lee BC, et al. A Comprehensive Human Gastric Cancer Organoid Biobank Captures Tumor Subtype Heterogeneity and Enables Therapeutic Screening. Cell Stem Cell. 2018; 23:882–897.e11.
https://doi.org/10.1016/j.stem.2018.09.016
PMID:30344100

28. Navin N, Krasnitz A, Rodgers L, Cook K, Meth J, Kendall J, Riggs M, Eberling Y, Troge J, Grubor V, Levy D, Lundin P, Månér S, et al. Inferring tumor progression from genomic heterogeneity. Genome Res. 2010; 20:68–80.
https://doi.org/10.1101/gr.099622.109
PMID:19903760

29. Li XC, Wang MY, Yang M, Dai HJ, Zhang BF, Wang W, Chu XL, Wang X, Zheng H, Niu RF, Zhang W, Chen KX. A mutational signature associated with alcohol consumption and prognostically significantly mutated driver genes in esophageal squamous cell carcinoma. Ann Oncol. 2018; 29:938–44.
https://doi.org/10.1093/annonc/mdy011
PMID:29351612

30. Sowalsky AG, Ye H, Bhasin M, Van Allen EM, Loda M, Lis RT, Montaser-Kouhsari L, Calagua C, Ma F, Russo JW, Schaefer RJ, Voznesensky OS, Zhang Z, et al. Neoadjuvant-Intensive Androgen Deprivation Therapy Selects for Prostate Tumor Foci with Diverse Subclonal Oncogenic Alterations. Cancer Res. 2018; 78:4716–30.
https://doi.org/10.1158/0008-5472.CAN-18-0610
PMID:29921690

31. Anagnostou V, Smith KN, Forde PM, Niknafs N, Bhattacharya R, White J, Zhang T, Adleff V, Phallen J, Wali N, Hruban C, Guthrie VB, Rodgers K, et al. Evolution of Neoantigen Landscape during Immune Checkpoint Blockade in Non-Small Cell Lung Cancer. Cancer Discov. 2017; 7:264–76.
https://doi.org/10.1158/2159-8290.CD-16-0828
PMID:28031159

32. Jamal-Hanjani M, Wilson GA, McGranahan N, Birkbak NJ, Watkins TB, Veeriah S, Shafi S, Johnson DH, Mitter R, Rosenthal R, Salm M, Horswell S, Escudero M, et al, and TRACERx Consortium. Tracking the Evolution of Non-Small-Cell Lung Cancer. N Engl J Med. 2017; 376:2109–21.
https://doi.org/10.1056/NEJMoa1616288
PMID:28445112

33. Huang K, Liu X, Li Y, Wang Q, Zhou J, Wang Y, Dong F, Yang C, Sun Z, Fang C, Liu C, Tan Y, Wu X, et al. Genome-Wide CRISPR-Cas9 Screening Identifies NF-κB/E2F6 Responsible for EGFRvIII-Associated Temozolomide Resistance in Glioblastoma. Adv Sci (Weinh). 2019; 6:1900782.
https://doi.org/10.1002/advs.201900782
PMID:31508283

34. Johnson BE, Mazor T, Hong C, Barnes M, Aihara K, McLean CY, Fouse SD, Yamamoto S, Ueda H, Tatsuno K, Asthana S, Jalbert LE, Nelson SJ, et al. Mutational analysis reveals the origin and therapy-driven evolution of recurrent glioma. Science. 2014; 343:189–93.
https://doi.org/10.1126/science.1239947
PMID:24336570

35. Hu H, Mu Q, Bao Z, Chen Y, Liu Y, Chen J, Wang K, Wang Z, Nam Y, Jiang B, Sa JK, Cho HJ, Her NG, et al. Mutational Landscape of Secondary Glioblastoma Guides MET-Targeted Trial in Brain Tumor. Cell. 2018; 175:1665–1678.e18.
https://doi.org/10.1016/j.cell.2018.09.038
PMID:30343896

36. Siegel RL, Miller KD, Jemal A. Cancer Statistics, 2017. CA Cancer J Clin. 2017; 67:7–30.
https://doi.org/10.3322/caac.21387 PMID:28055103

37. Cahill DP, Levine KK, Betensky RA, Codd PJ, Romany CA, Reavie LB, Batchelor TT, Futreal PA, Stratton MR, Curry WT, Iafrate AJ, Louis DN. Loss of the mismatch repair protein MSH6 in human glioblastomas is associated with tumor progression during temozolomide treatment. Clin Cancer Res. 2007; 13:2038–45.
https://doi.org/10.1158/1078-0432.CCR-06-2149
PMID:17404084

38. Wang J, Cazzato E, Ladewig E, Frattini V, Rosenbloom DI, Zairis S, Abate F, Liu Z, Elliott O, Shin YJ, Lee JK, Lee IH, Park WY, et al. Clonal evolution of glioblastoma under therapy. Nat Genet. 2016; 48:768–76.
https://doi.org/10.1038/ng.3590 PMID:27270107

39. Bender E. Trials show delayed recurrence in ovarian cancer. Cancer Discov. 2013; 3:OF8.
https://doi.org/10.1158/2159-8290.CD-ND2013-013
PMID:23749546

40. Newman AM, Bratman SV, To J, Wynne JF, Eclov NC, Modlin LA, Liu CL, Neal JW, Wakelee HA, Merritt RE, Shrager JB, Loo BW Jr, Alizadeh AA, Diehn M. An ultrasensitive method for quantitating circulating tumor DNA with broad patient coverage. Nat Med. 2014; 20:548–54.
https://doi.org/10.1038/nm.3519 PMID:24705333

41. Stroun M, Lyautey J, Lederrey C, Olson-Sand A, Anker P. About the possible origin and mechanism of

circulating DNA apoptosis and active DNA release. Clin Chim Acta. 2001; 313:139–42. https://doi.org/10.1016/S0009-8981(01)00665-9 PMID:11694251

42. Stroun M, Anker P. Nucleic acids spontaneously released by living frog auricles. Biochem J. 1972; 128:100P–01P. https://doi.org/10.1042/bj1280100pb PMID:4634816

43. Schwarzenbach H, Hoon DS, Pantel K. Cell-free nucleic acids as biomarkers in cancer patients. Nat Rev Cancer. 2011; 11:426–37. https://doi.org/10.1038/nrc3066 PMID:21562580

44. Martínez-Ricarte F, Mayor R, Martínez-Sáez E, Rubio-Pérez C, Pineda E, Cordero E, Cicuéndez M, Poca MA, López-Bigas N, Ramon Y Cajal S, Vieito M, Carles J, Tabernero J, et al. Molecular diagnosis of diffuse gliomas through sequencing of cell-free circulating tumour DNA from cerebrospinal fluid. Clin Cancer Res. 2018; 24:2812–19. https://doi.org/10.1158/1078-0432.CCR-17-3800 PMID:29615461

45. Przybyl J, Chabon JJ, Spans L, Ganjoo KN, Vennam S, Newman AM, Forgó E, Varma S, Zhu S, Debiec-Rychter M, Alizadeh AA, Diehn M, van de Rijn M. Combination Approach for Detecting Different Types of Alterations in Circulating Tumor DNA in Leiomyosarcoma. Clin Cancer Res. 2018; 24:2688–99. https://doi.org/10.1158/1078-0432.CCR-17-3704 PMID:29463554

46. Tie J, Wang Y, Tomasetti C, Li L, Springer S, Kinde I, Silliman N, Tacey M, Wong HL, Christie M, Kosmider S, Skinner I, Wong R, et al. Circulating tumor DNA analysis detects minimal residual disease and predicts recurrence in patients with stage II colon cancer. Sci Transl Med. 2016; 8:346ra92. https://doi.org/10.1126/scitranslmed.aaf6219 PMID:27384348

47. Abbosh C, Birkbak NJ, Wilson GA, Jamal-Hanjani M, Constantin T, Salari R, Le Quesne J, Moore DA, Veeriah S, Rosenthal R, Marafioti T, Kirkizlar E, Watkins TB, et al, and TRACERx consortium, and PEACE consortium. Phylogenetic ctDNA analysis depicts early-stage lung cancer evolution. Nature. 2017; 545:446–51. https://doi.org/10.1038/nature22364 PMID:28445469

48. Heitzer E, Haque IS, Roberts CES, Speicher MR. Current and future perspectives of liquid biopsies in genomics-driven oncology. Nat Rev Genet. 2019; 20:71–88. https://doi.org/10.1038/s41576-018-0071-5 PMID:30410101

49. Jiang T, Mao Y, Ma W, Mao Q, You Y, Yang X, Jiang C, Kang C, Li X, Chen L, Qiu X, Wang W, Li W, et al, and Chinese Glioma Cooperative Group (CGCG). CGCG clinical practice guidelines for the management of adult diffuse gliomas. Cancer Lett. 2016; 375:263–73. https://doi.org/10.1016/j.canlet.2016.01.024 PMID:26966000

50. Bindea G, Mlecnik B, Hackl H, Charoentong P, Tosolini M, Kirilovsky A, Fridman WH, Pagès F, Trajanoski Z, Galon J. ClueGO: a Cytoscape plug-in to decipher functionally grouped gene ontology and pathway annotation networks. Bioinformatics. 2009; 25:1091–93. https://doi.org/10.1093/bioinformatics/btp101 PMID:19237447

51. Cibulskis K, Lawrence MS, Carter SL, Sivachenko A, Jaffe D, Sougnez C, Gabriel S, Meyerson M, Lander ES, Getz G. Sensitive detection of somatic point mutations in impure and heterogeneous cancer samples. Nat Biotechnol. 2013; 31:213–19. https://doi.org/10.1038/nbt.2514 PMID:23396013

52. Saunders CT, Wong WS, Swamy S, Becq J, Murray LJ, Cheetham RK. Strelka: accurate somatic small-variant calling from sequenced tumor-normal sample pairs. Bioinformatics. 2012; 28:1811–17. https://doi.org/10.1093/bioinformatics/bts271 PMID:22581179

53. Boeva V, Popova T, Bleakley K, Chiche P, Cappo J, Schleiermacher G, Janoueix-Lerosey I, Delattre O, Barillot E. Control-FREEC: a tool for assessing copy number and allelic content using next-generation sequencing data. Bioinformatics. 2012; 28:423–25. https://doi.org/10.1093/bioinformatics/btr670 PMID:22155870

54. Layer RM, Chiang C, Quinlan AR, Hall IM. LUMPY: a probabilistic framework for structural variant discovery. Genome Biol. 2014; 15:R84. https://doi.org/10.1186/gb-2014-15-6-r84 PMID:24970577

55. Alexandrov LB, Nik-Zainal S, Wedge DC, Campbell PJ, Stratton MR. Deciphering signatures of mutational processes operative in human cancer. Cell Rep. 2013; 3:246–59. https://doi.org/10.1016/j.celrep.2012.12.008 PMID:23318258

56. Wendl MC, Wallis JW, Lin L, Kandoth C, Mardis ER, Wilson RK, Ding L. PathScan: a tool for discerning mutational significance in groups of putative cancer genes. Bioinformatics. 2011; 27:1595–602. https://doi.org/10.1093/bioinformatics/btr193 PMID:21498403

SUPPLEMENTARY MATERIALS

Supplementary Figures

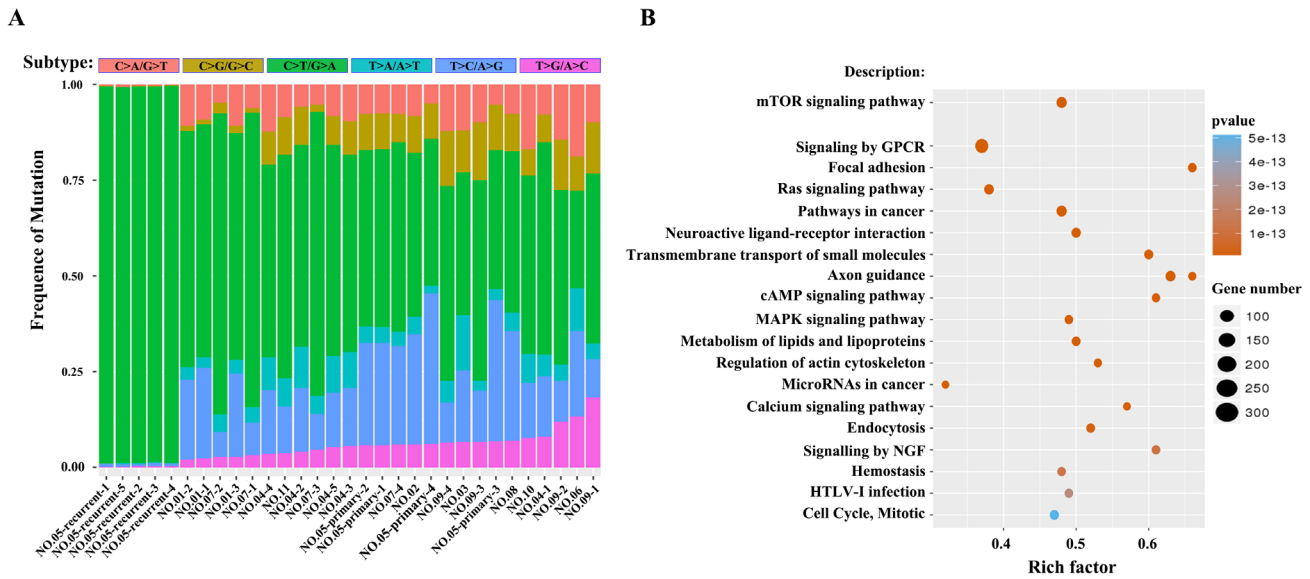

Supplementary Figure 1. (**A**) The abscissa indicates the sample name, the ordinate indicates the proportion of each mutation type in the sample, and different colors represent different SNV mutation types. (**B**) Pathway analysis of SMGs. The ordinate provides the pathway description, the abscissa lists the gene detection rate in each pathway, the size of the dot represents the number of genes in each pathway and the color of the dot represents the range of p values.

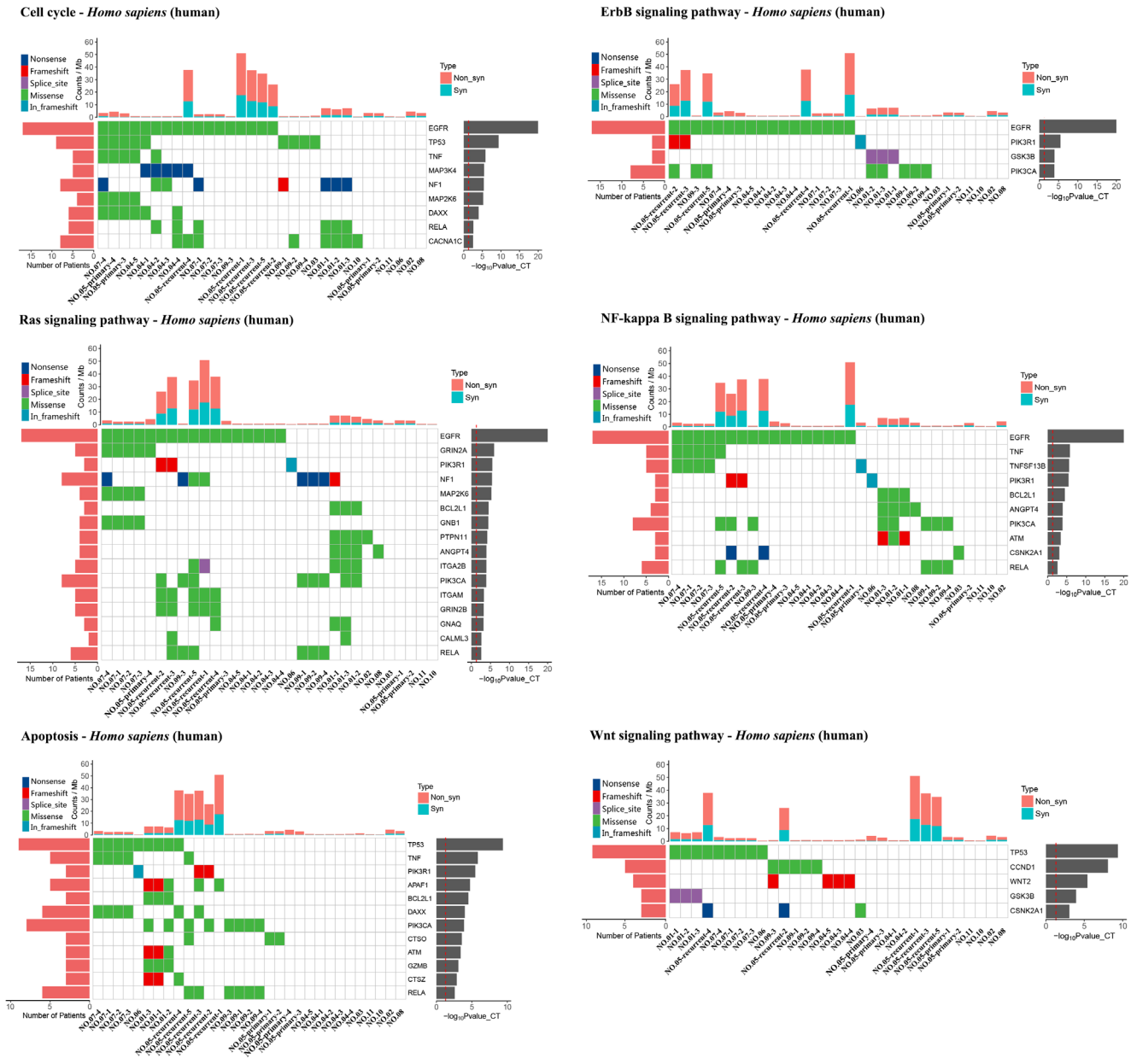

Supplementary Figure 2. Significantly mutated genes (SMGs) involved in the cell cycle, ErbB signaling, RAS signaling, NF-kappa signaling, apoptosis and the wnt signaling pathway. The graph on the right presents the log10 P-value of each gene mutation. The heat map (middle panel) presents gene mutations in GBM samples. The graph on the left shows the mutation frequency in the GBM samples examined. The mutant load is shown on top of the heat map.

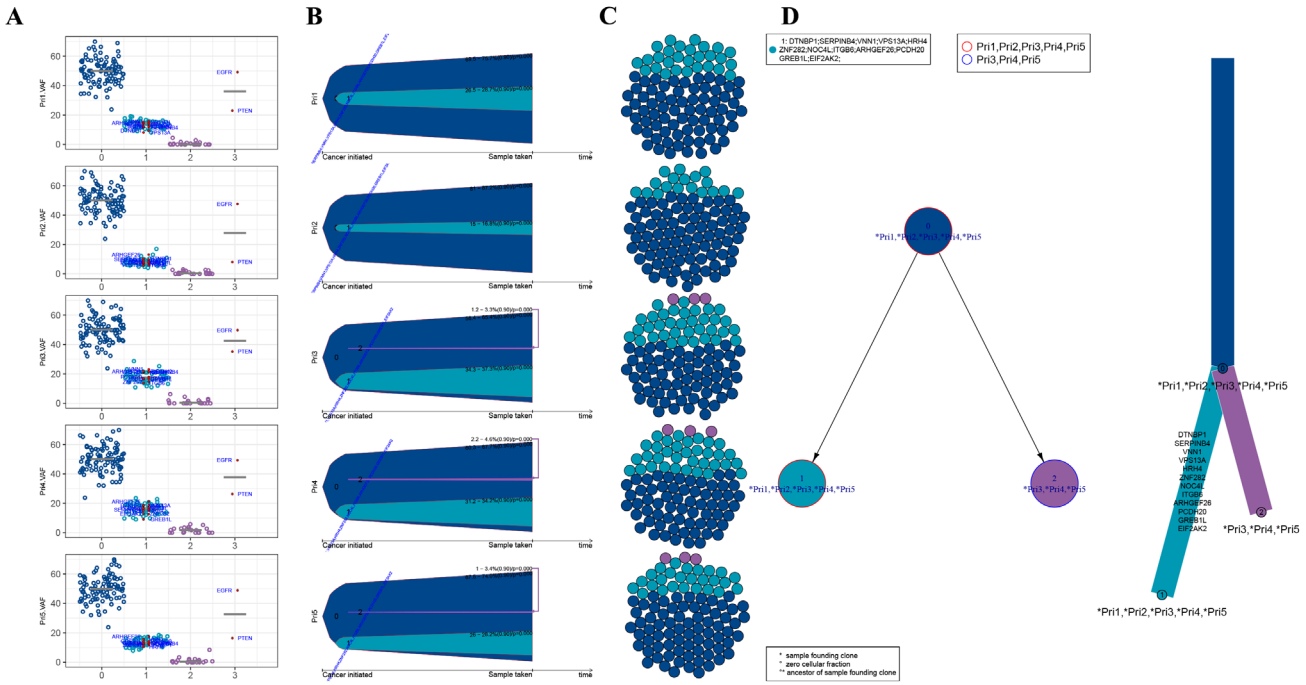

Supplementary Figure 3. Analysis of the subclones and evolution of GBM samples from patient NO. 04.

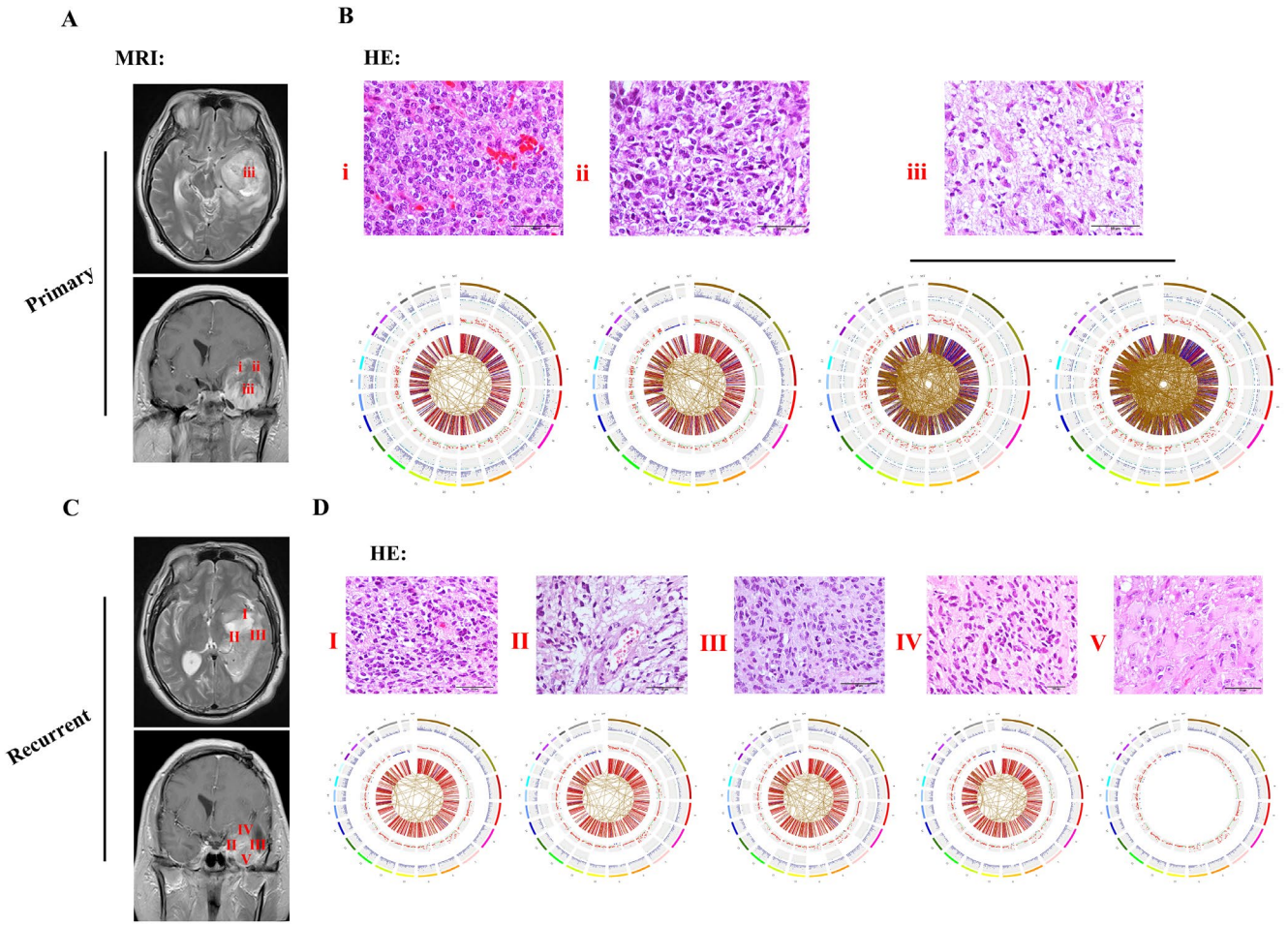

Supplementary Figure 4. (**A**) Magnetic resonance images of the primary glioblastoma tumor from patient NO. 05. (**i**, **ii**, and **iii**) indicate the locations of the multipoint samples. (**B**) HE staining and genome mutation circos plots of primary multipoint samples from patient NO. 05. The first circle indicates chromosomes. The dark purple dots in the second circle represent the density of SNPs, The dark blue points in the third circle denote the density of INDELs. The fourth circle presents the CNV results, where red indicates an increased copy number, blue indicates a decreased copy number, and green indicates a normal copy number. The fifth circle presents the SV results. Due to the large amount of data, only SV data from exons and splice sites are displayed: CTX (brown), ITX (blue), INS (orange), DEL (dark red), DUP (light purple) and INV (green). (**C**) Magnetic resonance images of the recurrent tumors from patient NO. 05. (**I**-**V**) indicate the locations of the multi-point samples. (**D**) HE staining and genome mutation circos plots of recurrent multipoint samples from patient NO. 05.

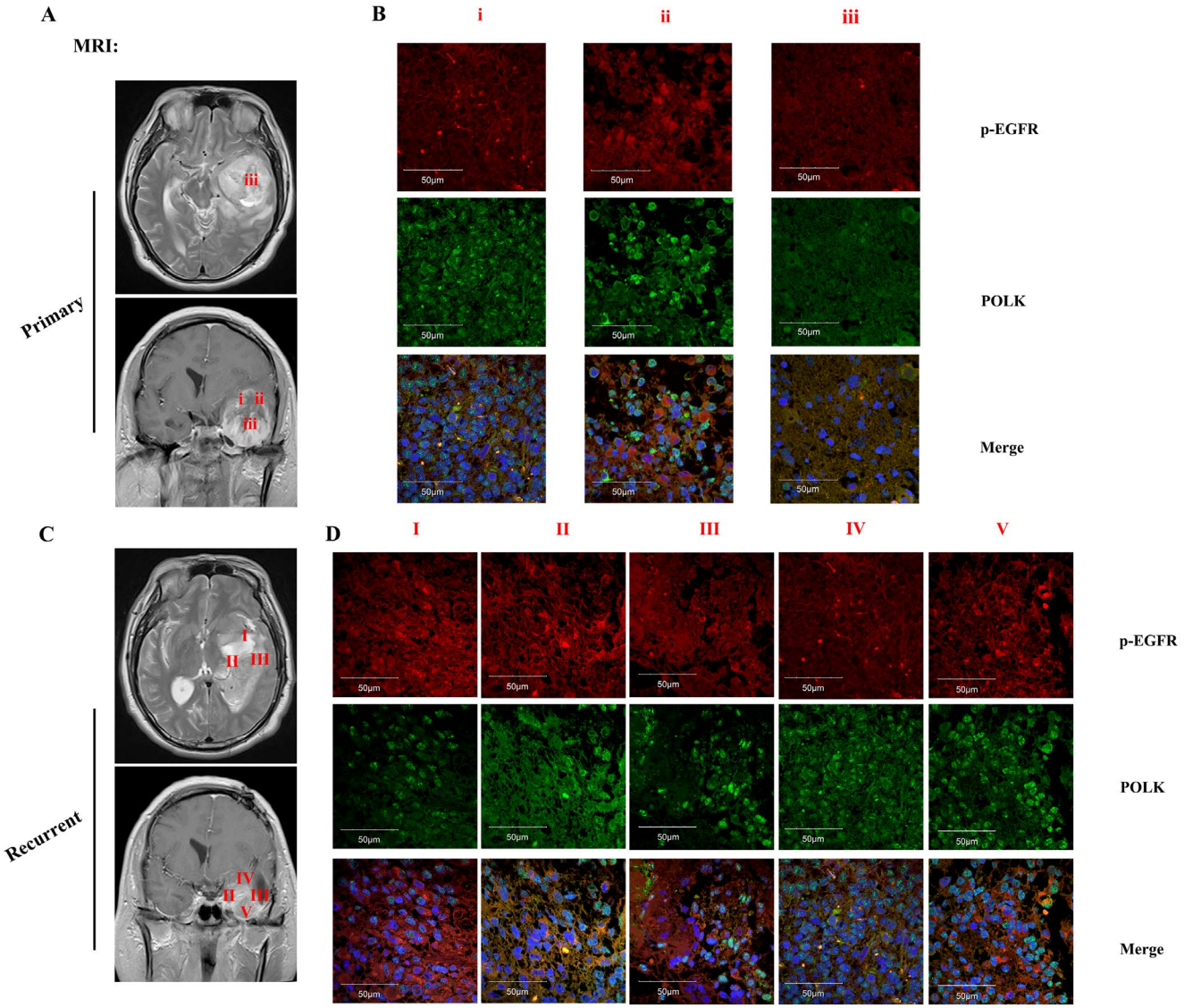

Supplementary Figure 5. (**A**) Magnetic resonance images of the primary glioblastoma tumors from patient NO. 05. (**i**–**iii**) indicate the locations of the multi-point samples. (**B**) Immunofluorescence staining of primary multipoint samples from patient NO. 05. (**C**) Magnetic resonance images of the recurrent tumors from patient NO. 05. (**I**–**V**) indicate the locations of the multi-point samples. (**D**) Immunofluorescence staining of recurrent multipoint samples from patient NO. 05.

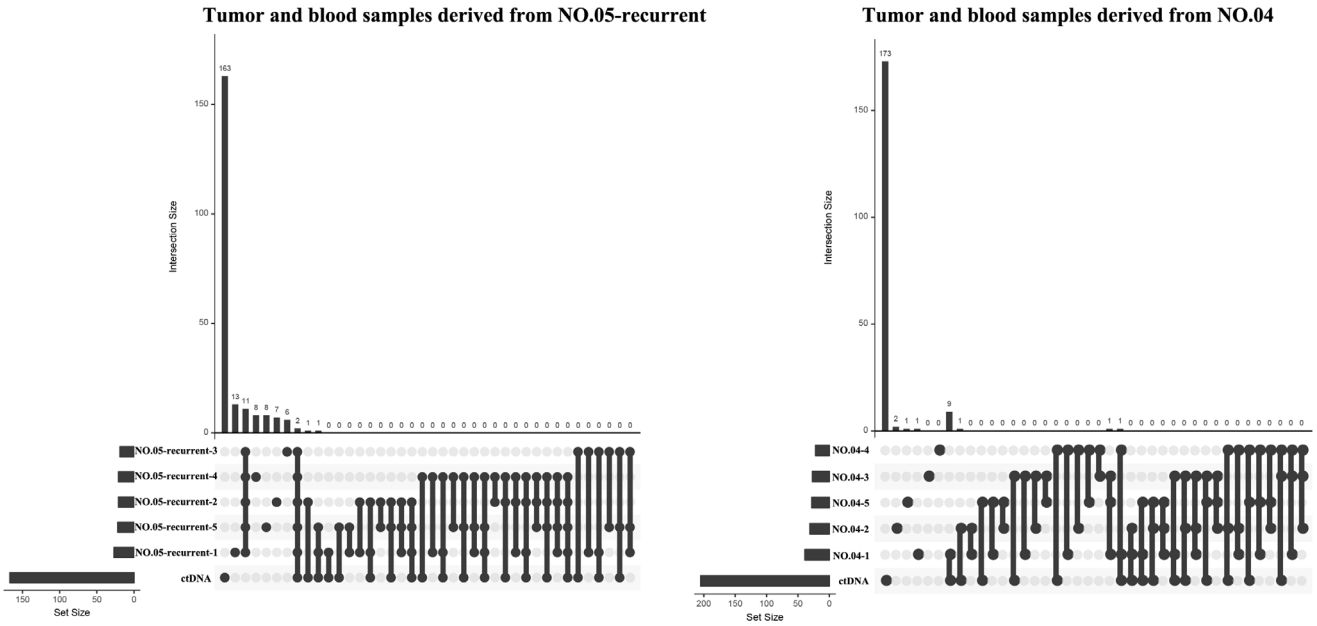

Supplementary Figure 6. Results of the ctDNA test and statistical analysis of the same mutations in the region of the ctDNA sequenced identified using exon sequencing at different tumor sites from patients NO. 05-recurrent and NO. 04.

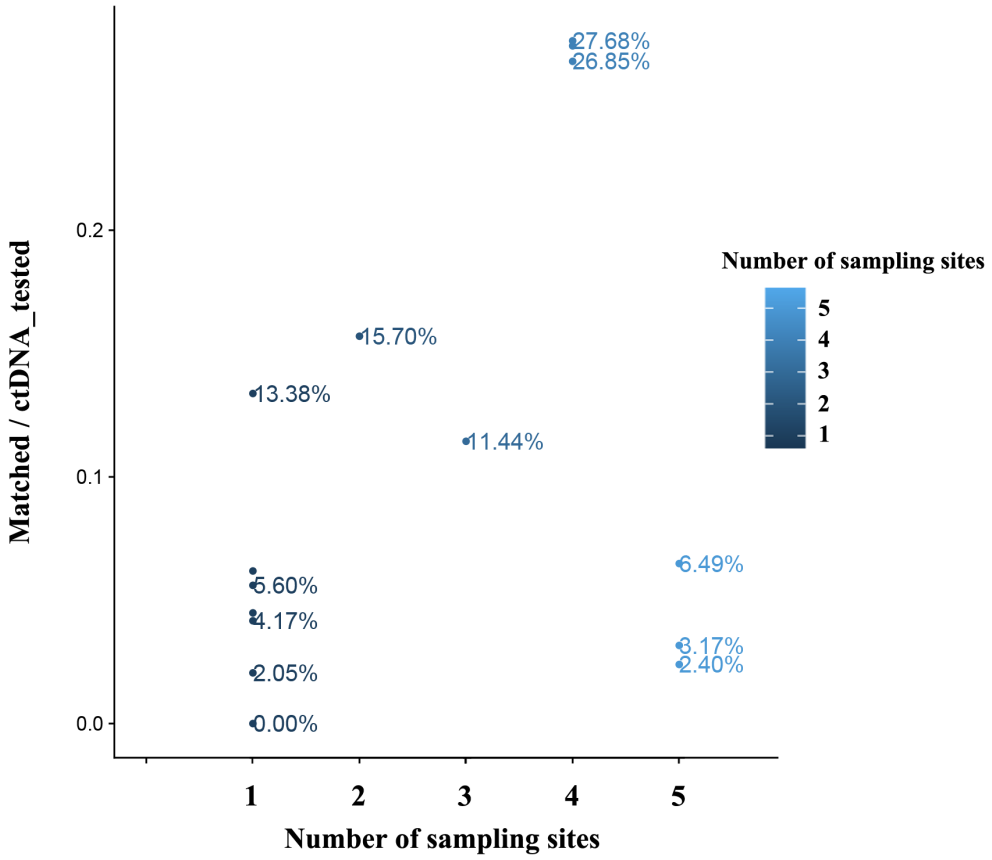

Supplementary Figure 7. Matching probability of ctDNA test and exon sequencing data in the region of the ctDNA sequenced from each patient.

Supplementary Table

Supplementary Table 1. Clinical data for the tumor samples

ID	Age	Gender	Sample type	Number of samples
NO.01	62	male	rGBM	3
NO.02	56	female	GBM	1
NO.03	51	female	GBM	1
NO.04	66	male	GBM	5
NO.05	45	male	GBM	4
NO.05-recurrent	46	male	rGBM	5
NO.06	19	male	GBM	1
NO.07	32	male	GBM	4
N0.08	62	male	GBM	1
N0.09	70	male	GBM	4
NO.10	61	male	GBM	1
NO.11	64	male	GBM	1